Crimson Publishers
Wings to the Research

Research Article

Photoactive Bioconjugates of R-phycoerythrin with Ag^0 and CdS Nanoparticles: Trehalose-Induced Changes in Properties

Bekasova OD*

Bach Institute of Biochemistry, Federal Research Centre Fundamentals of Biotechnology, Russian Academy of Sciences, Russia

ISSN: 2637-8078

***Corresponding author:** Bekasova OD, Bach Institute of Biochemistry, Federal Research Centre Fundamentals of Biotechnology, Russian Academy of Sciences, Russia

Submission: October 04, 2022
Published: October 28, 2022
Volume 5 - Issue 5

How to cite this article: Bekasova OD*. Photoactive Bioconjugates of R-phycoerythrin with Ag^0 and CdS Nanoparticles: Trehalose-Induced Changes in Properties. Significances of Bioengineering & Biosciences. 5(5). SBB. 000621. 2022.
DOI: 10.31031/SBB.2022.05.000621

Copyright@ Bekasova OD, This article is distributed under the terms of the Creative Commons Attribution 4.0 International License, which permits unrestricted use and redistribution provided that the original author and source are credited.

Abstract

A comparative study was performed for the effect of trehalose on two photo bioconjugates of R-Phycoerythrin (PE) with nanoparticles (NPs) of similar size but different nature. Light-sensitive bioconjugates of PE with Ag^0 and CdS NPs (Ag^0-PE and CdS-PE) show promise for recording intermolecular interactions, cancer theranostics and drug delivery due to their unique optical properties, ability of ROS generation, electrical activity, and small size. Bioconjugates were obtained by synthesizing Ag^0 and CdS NPs in the tunnel cavities of R-phycoerythrin, a photosynthetic pigment of red algae, as a natural resource. The current study was undertaken to determine the influence of trehalose, a known protein stabilizer, on the properties of Ag^0·PE and CdS·PE bioconjugates. The results indicate that the fluorescence intensity of both bioconjugates increases when excited by visible light. However, the mechanisms of their fluorescence enhancement are different. The intensity of CdS·PE fluorescence excited at 280nm decreases in the presence of trehalose by about half, while the fluorescence of Ag^0·PE remains unchanged. The ambiguous effect of trehalose on the UV-excited fluorescence of Ag^0·PE and CdS·PE bioconjugates is due to the unequal nature of NPs (metallic and semiconducting) is discussed. Trehalose has no effect on the size of NPs in both bioconjugates. Trehalose inhibits the ability of R-phycoerythrin to photosensitize the electron transfer. It was demonstrated that trehalose can be successfully used in rapidly developing nanotechnology based on photo bioconjugates as a promising source of multifunctional biomaterials and highly sensitive optical biosensor systems.

Keywords: Nanotechnology; Photoactive bioconjugates; R-phycoerythrin; Silver nanoparticles; Semiconductor nanoparticles

Abbreviations: PE: R-phycoerythrin; NPs: Nanoparticles; Ag^0·PE: Bioconjugate of R-phycoerythrin with Ag^0 nanoparticle; CdS·PE: Bioconjugate of R-phycoerythrin with CdS nanoparticle; ROS: Reactive Oxygen Species; Trp: Tryptophan

Introduction

Bioactive materials for nanomedicine and highly sensitive electrochemical and optical biosensor systems for the diagnosis and monitoring of diseases are in high demand [1-3]. Composites of photoactive biomolecules with metallic or semiconductor Nanoparticles (NPs) are regarded as a promising source of multifunctional biomaterials for simultaneous cancer diagnosis and treatment, devices simulating the functions of various cells, and highly sensitive biosensor systems [4]. Preference is given to multifunctional nanostructures derived from natural resources. Biosynthesized NPs cause low toxicity, have high biocompatibility, are used in lower concentrations, and have fewer unwanted side effects, as compared to NPs produced by chemical synthesis [5]. In view of this, we studied photoactive bioconjugates, which were obtained by synthesizing Ag^0 NPs and CdS NPs in the tunnel cavities of R-phycoerythrin molecules, a photosynthetic pigment in red algae, as a natural resource. The main function of R-phycoerythrin is the absorption of solar energy and its transfer to the reaction centers of Photosystem II. R-Phycoerythrin is a high-molecular-weight protein containing linear tetrapyrrole chromophores, Phycoerythrobilun (PEB) and Phycourobilin (PUB) [6]. R-Phycoerythrin is compose of α and β subunits that form either trimer $(\alpha\beta)_3$ or hexamer $(\alpha\beta)_6$. Native R-phycoerythrin is a hexamer consisting of face-to-face stacked disc-shaped trimers $(\alpha\beta)_3$ 10-12nm in diameter and 3nm high [7,8].

The tunnel cavity of 3.5nm in diameter is in the center of each R-phycoerythrin molecule $(\alpha\beta)_6$. R-Phycoerythrin exhibits strong absorption in the visible range and emits fluorescence (maximum at 578nm; excitation lifetime, 2.9ns; quantum yield, 0.9) [9]. R-Phycoerythrin is capable to generate free radicals and reactive oxygen species (ROS) under illumination [10]. Along with other phycobiliproteins, R-phycoerythrin is successfully used in food industry as a colorant, in photodynamic therapy of cancer and skin diseases, as a generator of ROS, and as a fluorescent label in cytometry, histochemistry, and immunoassays [11-13]. R-Phycoerythrin subunits and chromophore-containing peptides show good potential for use as fluorescent probes for single-molecule detection and single-cell analysis [14]. We used R-phycoerythrin as a matrix to obtain NPs [15-17]. The advantages of R-phycoerythrin as a matrix for the synthesis of NPs include the identical size of tunnel cavities (3.5×6.0nm) in the center of all molecules, high solubility in water, and the absence of toxicity. Nanoparticles synthesized in R-phycoerythrin have properties useful for their practical applications [18]. In particular, Ag^0 NPs inhibit thermal aggregation of R-phycoerythrin and have high electrical conductivity [19-21]. The trend and magnitude of the dielectric and electrical properties of Ag^0·PE are of the same order as that of composites of conductive polymers with metallic nanowires [22,23]. Ag^0 NPs prepared by green synthesis exhibit anticancer activity [24,25]. Choi et al. [26] used R-phycoerythrin used to synthesize reduced graphene oxide-silver nanoparticle nanocomposites (RPE-rGO-Ag), which showed significant toxicity towards both ovarian cancer cells and ovarian cancer stem cells. Besides, RPE-rGO-Ag enhances cytotoxic and apoptotic potential of salinomycin in human ovarian cancer stem cells.

Ag^0 NPs and CdS NP synthesized in R-phycoerythrin show intense fluorescence. The fluorescence lifetimes (τ) of single Ag^0 NPs in the R-phycoerythrin matrix are τ_1=0.18ns, τ_2=2.8ns in solution and τ_1=0.45ns, τ_2=2.4 ns on the glass surface [27]. The fluorescence lifetimes of single CdS·PE are τ_1=0.26ns, τ_2=1.9ns in solution and τ_1=0.83ns, τ_2=3.3 ns on the glass surface [28]. Therefore, Ag^0 PE and CdS PE bioconjugates, along with other bioconjugates prepared from light-sensitive biomolecules with noble metal NPs and semiconductor NPs, may be very useful for creating new optoelectronic devices and have potential for theranostic applications in medicine. For example, biogenic Ag^0 NPs have demonstrated the ability to fluoresce [24] but Ag^0 NPs synthesized in R-phycoerythrin emit red fluorescence even more intensively due to properties of R-phycoerythrin, as a photosensitizer. Cancer cells upon treatment with biogenic Ag^0 NPs emitted bright red fluorescence while untreated cells used as control and those treated which chemically synthesized Ag^0 NPs did not emit red fluorescence [24]. Numerous researchers suggest that the anti-cancer activity of biogenic Ag NPs is observed due to the formation of ROS inside cancer cells. ROS is ultimately responsible for cellular damage [25]. Note that free R-phycoerythrin and in combination with Ag^0 NPs or CdS NPs also are capable of generating ROS and exhibits anti-cancer activity.

CdS NPs in R-phycoerythrin are photochemically active and have a strong photoelectric effect similar to that of 6-9nm CdS NPs synthesized on the surface of single-walled carbon nanotubes [29,30]. It should be emphasized that Ag^0·PE and CdS·PE bioconjugates are highly soluble in water and have a relatively large surface area suitable for modification by the functional groups with different chemical and biochemical properties. An important requirement for bioactive materials is their high stability. Trehalose, a nonreducing disaccharide consisting of two cyclic D-glucose units linked together by a glycosidic bond, which is responsible for its high stability, possesses an extraordinary ability to stabilize biological molecules. Many hypotheses have been advanced to explain the exceptional ability of trehalose to stabilize biological molecules, but a unified theory has not yet emerged, and the mechanism of this phenomenon is still unclear. It is known, however, that trehalose stabilizes denatured proteins and thereby prevents their aggregation. The protective action of trehalose under UV-irradiation is based on prolongation the nucleation phase and reduces the rate of structural reorganization of irradiated protein molecules [31]. Trehalose is widely used to enhance protein stability and is applied mainly in the food, cosmetic and pharmaceutical industries. The effect of trehalose on proteins in heterostructures with NPs has been little studied, while stable bioactive materials are in great demand. In view of this, the aim of this study was to investigate the effect of trehalose on the fluorescence emission and photosensitizing activity of R-phycoerythrin in bioconjugates with NPs produced in the central cavity of R-phycoerythrin hexamers. Note that the properties of bioconjugates such as fluorescence and the ability to photosensitize various reactions, important properties. The results of this study may lead to the use of trehalose in nanotechnologies based on photobioconjugates.

Materials and Methods

Isolation and purification of R-phycoerythrin

R-Phycoerythrin was isolated from the marine red alga Callithamnion rubosum. The procedure involved the extraction with distilled water for 8h, concentration by precipitation with ammonium sulfate, and chromatography on hydroxyapatite and Sephadex G-200 columns in 0.06M phosphate buffer, pH 6.8. The purified protein was dialyzed against distilled water for 24h, lyophilized, and stored in vacuum at 8 °C as described previously [19]. Immediately before experiments, R-phycoerythrin was dissolved in Milli-Q water, centrifuged at 16,000rpm for 10min, and dialyzed against Milli-Q water for 12h at 8 °C. The purity of the preparations was assessed from the ratio of the absorbance at 563, 496 and 280nm. For pure R-phycoerythrin in our preparations, D_{563}/D_{280}=4.6, D_{563}/D_{496}=1.2. The concentration of R-phycoerythrin was measured spectrophotometrically at 563nm using the extinction coefficient $A^{1\%}_{563} = 0.82$ [32].

Preparation of the Ag^0·PE bioconjugate by green synthesis of Ag^0NPs in tunnel cavities of R-phycoerythrin

We used the R-phycoerythrin hexamers for the simple and cost-

Copyright © Bekasova OD

effective green synthesis of Ag^0NPs. In this process, R-phycoerythrin served not only as a reducing agent but also as a matrix for Ag^0NPs. The synthesis was initiated by adding 0.3M $AgNO_3$ to a 2.8μM R-phycoerythrin solution in Milli-Q water to the final concentration of 6.0mM Ag^+, as described previously [17]. This concentration was chosen based on the preliminary experiments, in which the conditions for the preparation of stable Ag^0NPs in a dispersed phase were optimized. The R-phycoerythrin solution was incubated with silver ions for 7-10h at 8 °C and then centrifuged at 12,000rpm for 10min at 4 °C. The precipitate was discarded, and the supernatant was chromatographed on a Sephadex G-25 column to remove free Ag^+ ions and stored at 8 °C for 2-3 months. Each Ag^0·PE sample was centrifuged at 12,000rpm for 10min at 4 °C and examined by absorption and fluorescence spectroscopy immediately before use in experiments. The R-phycoerythrin concentration in the Ag^0·PE bioconjugate was determined by the Bradford method using Coomassie brilliant blue G-250 (Serva, Germany) [33].

Preparation of CdS·PE bioconjugate by two-step synthesis of CdS NP in the tunnel cavity of R-phycoerythrin

The synthesis of CdS NPs in the central tunnel cavities of the R-phycoerythrin hexamers was performed as described in [15,16] but using a lower initial concentration of the protein. The synthesis was initiated by adding 0.5M $Cd(NO_3)_2$ to a 0.4μM R-phycoerythrin solution in Milli-Q water to the final concentration of 6mM Cd^{2+}. The formation of the Cd/R-phycoerythrin complex was monitored potentiometrically by measuring the changes in the equilibrium concentration of Cd^{2+} using an Expert-001pH/millivoltmeter (Russia) equipped with an Ecom-Cd electrode selective for Cd^{2+}. Upon binding of Cd^{2+}, the water solubility of R-phycoerythrin remained high. Thereafter, 0.3M Na_2S was added to the final concentration of 9.1mM S^{2-}, and the mixture was incubated for 30min and centrifuged at 3000rpm for 10min. The supernatant contained R-phycoerythrin with CdS NPs synthesized in the tunnel cavities, which was additionally purified by gel filtration on a Sephadex G-200 column. Our observations showed that CdS NPs synthesized in R-phycoerythrin remained stable for several months. The location of CdS NPs in the tunnel cavities of R-phycoerythrin molecules was confirmed in our previous studies by different methods, including capillary electrophoresis and analytical ultracentrifugation [15,28]. The size of CdS NPs was estimated from the absorption spectra using the plot of the band gap (exciton energy) versus the particle size [34] and from TEM images.

Transmission electron microscopy (TEM)

Transmission electron microscopy was used to determine the sizes of bioconjugates and NPs. A drop of the sample (5μg/mL) was applied on a copper grid coated with a Formvar film, contrasted with 2% phosphotungstic acid, pH 7.2 (to detect R-phycoerythrin) or not contrasted (to detect NPs), air-dried, and examined using a JEM-100CX TEM (JEOL, Japan) operating at 80kV and a nominal magnification of 30,000×. Besides, in order to characterize the elemental composition of the NP, some specimens were prepared by freezing. The elemental composition of the NPs was determined by energy-dispersive electron probe X-ray microanalysis at 25kV on a Tesla BS-540 TEM (Czech Republic) equipped with a Ge-Li detector.

Spectroscopy

The UV-VIS absorption spectra were measured on a UV-1601PC spectrophotometer (Shimadzu, Japan) in a 1cm pathlength cuvette. Fluorescence spectra of samples, which were placed in a 0.2cm pathlength cuvette, were recorded on a RF-5301PC spectrofluorometer (Shimadzu, Japan) equipped with an R928-08 photomultiplier sensitive in the long-wavelength region.

Potentiometry

Potentiometric measurements were performed with an accuracy of 1-2mV on a device consisting of an LPU-01 potentiometer (Russia), an OI-18 mercury lamp illuminator with an operating current of 1.1-1.2 A (OMO, Russia), and a two-compartment cell with platinum and calomel electrodes [29]. To make preparations (solid films) for these measurements, the test solution (native R-phycoerythrin or CdS·PE in deionized water or CdS·PE in 0.73M trehalose) was placed as a hanging drop onto a platinum electrode (0.3×0.3cm) and dried in the dark at room temperature and atmospheric pressure. All measurements were performed in triplicate.

Results

TEM images of Ag^0·PE and CdS·PE bioconjugates

R-phycoerythrin is clearly visible in TEM images of Ag^0·PE and CdS·PE bioconjugates contrasted with 2% phosphotungstic acid, (Figure 1). According to the results of electron microscopy, R-phycoerythrin and its conjugates with Ag^0 NPs or CdS NPs are of similar size and disk-like shape 10-12nm in diameter. These parameters are the same as those of the native R-phycoerythrin [7]. Nanoparticles, unlike R-phycoerythrin, are clearly visible in TEM images of bioconjugates without contrast (Figure 2). The size of the predominant NPs in freshly prepared Ag^0·PE and CdS·PE was 6.5±0.5nm (Figure 2). This size is equal to the length of the R-phycoerythrin tunnel cavity. The elemental composition of the NPs was confirmed using characteristic energy-dispersive X-ray spectroscopy (Figure 3). The zero-valent state of silver is confirmed by the fact that the energy-dispersive X-ray spectrum of the Ag^0·PE sample shows a signal corresponding to Ag^0 (E=2.98keV), (Figure 3a).

Copyright © Bekasova OD

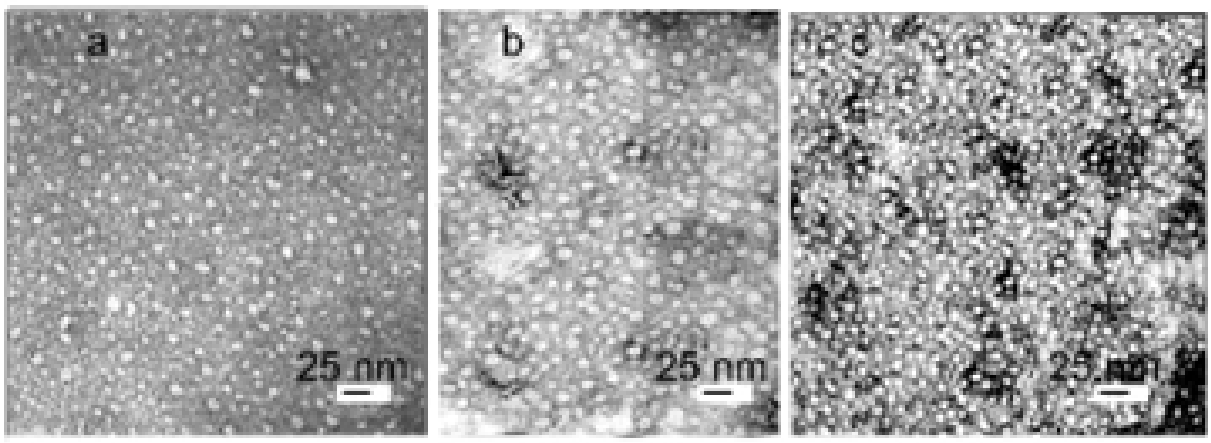

Figure 1: TEM micrographs of (a) R-phycoerythrin, (b) Ag^0·PE bioconjugate and (c) CdS·PE bioconjugate contrasted with 2% phosphotungstic acid, pH 7.2.

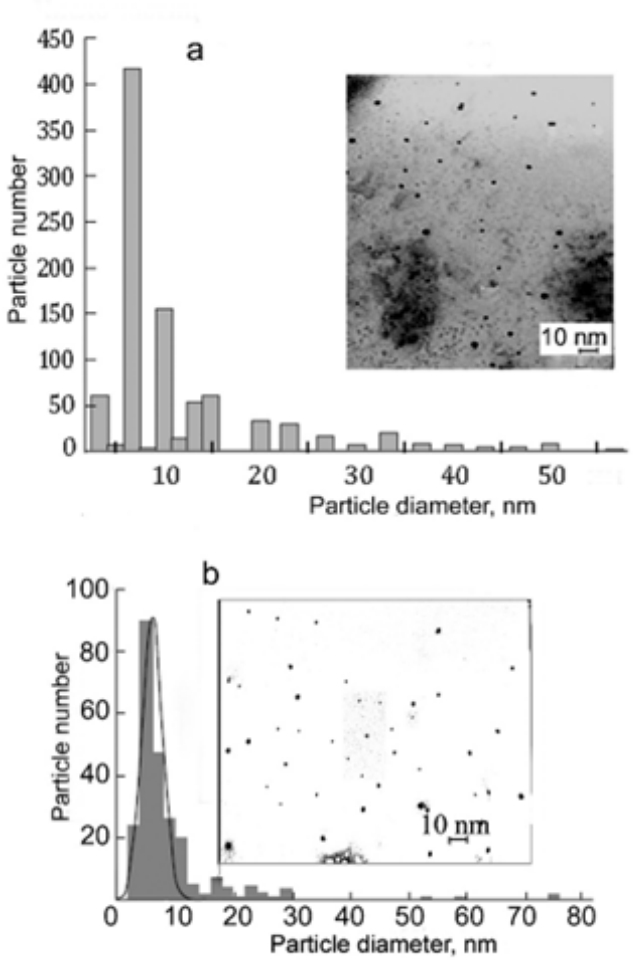

Figure 2: Graphs of the particle size distribution for bioconjugates:

a. Ag^0·PE and

b. CdS·PE in ultrapure water. The root-mean-square deviation is 1.82.

The inset electron micrographs show $Ag^0$and CdS NPs on images of (a) Ag^0·PE and (b) CdS·PE, respectively, without contrasting with phosphotungstic acid.

Copyright © Bekasova OD

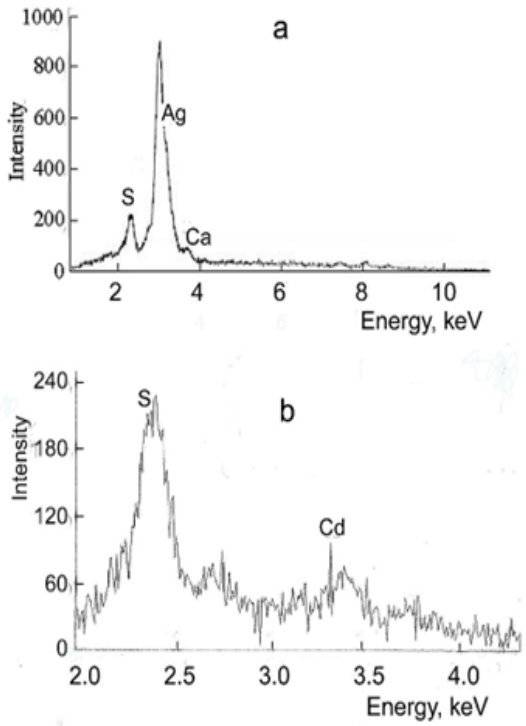

Figure 3: Energy-dispersive X-ray spectra of nanoparticles:
a. Ag^0 NPs and
b. CdS NPs synthesized in R-phycoerythrin in ultrapure water.

Optical properties of Ag^0·PE bioconjugate

The absorption spectrum of R-phycoerythrin has maxima at 498, 540, and 568nm (Figure 4a, curve 1). The filling of the tunnel cavity by Ag^0 NP caused changes in the absorption spectrum of R-phycoerythrin. As shown in Figure 4a, curve 2, the main peak in the absorption spectrum of Ag^0·PE is observed at 497nm and corresponds to the absorption maximum of PUB. The absorption peak at 568nm corresponding to PEB is absent in the absorption spectrum of Ag^0·PE. The structure of the absorption spectrum of Ag^0 NPs in the Ag^0·PE bioconjugate is masked by absorption of the pigment in the UV/blue spectral region. The absorption spectra of Ag^0·PE in the absence and in the presence of trehalose coincide with each other. Previously, we proved that R-phycoerythrin in the Ag^0·PE bioconjugate undergoes intramolecular cross-linking by Ag^0 NP [19]. Therefore, the absorption spectrum of Ag^0·PE is not affected by trehalose.

As is seen in Figure 4b, R-phycoerythrin emits high-intensity fluorescence with a maximum at 578nm (half-width 27nm) and a shoulder at 630nm.The shape of the fluorescence spectrum is independent of the excitation by photons with different energies. In contrast the fluorescence emission spectrum of Ag^0·PE is extremely sensitive to the exciting-photon energy. This is evidenced by the strong shift of the maximum in the bioconjugate fluorescence spectrum when the excitation wavelength changes (Figures 4b & 4c). The tryptophan fluorescence band with a maximum at 360nm dominates. This means that there is no intramolecular transfer of excitation energy due to changes in the distances between tryptophan residues and chromophore groups and their mobility as a result of intramolecular cross-linking of R-phycoerythrin by Ag^0 NPs. In addition, Ag^0, as a neutral molecule, is unable to tear off an electron from the indole ring of tryptophan when it is in the excited state, unlike CdS (see below). The fluorescence spectrum of the Ag^0 PE bioconjugate shows maxima at 450 and 510nm typical of silver NPs [35]. The fluorescence intensity of Ag^0 NPs synthesized and stabilized in a solution of R-phycoerythrin is an order of magnitude higher than the intensity in other matrices.

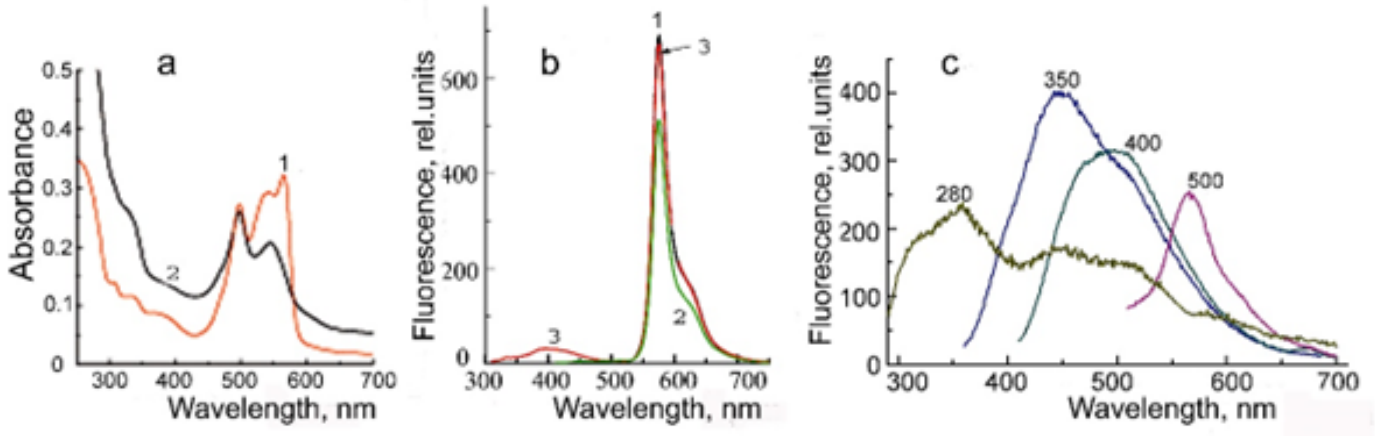

Figure 4: (a) Absorption spectra of R-phycoerythrin (curve 1) and Ag^0·PE (curve 2) in ultrapure water. (b) The fluorescence emission spectrum of R-phycoerythrin (1) excited at 500nm, (2) 400nm, and (3) 280 nm. (c) The fluorescence emission spectrum of Ag^0·PE. Numbers at the curves indicate the excitation wavelengths.

Copyright © Bekasova OD

The intensity of Ag^0·PE fluorescence excited by visible light increases in the presence of trehalose and the fluorescence spectrum components become more clear, especially at λ_{ex}=400nm (Figure 5). As shown in Figure 5a, the fluorescence spectrum of Ag^0·PE excited at 400nm in the absence of trehalose shows a broad band with a maximum at 480-510nm, while in the presence of trehalose the spectrum has a dominant peak with a maximum at 500nm and two shoulders at 575 and 450nm corresponding to R-phycoerythrin and Ag^0 NPs fluorescence, respectively. The changes in the fluorescence intensity at the maxima depending on the excitation wavelength in the absence and in the presence of trehalose are shown in Figure 5b. The changes in the total fluorescence emission of the Ag^0·PE bioconjugate at different excitation wavelengths under the influence of trehalose are summarized in the lowest line in Figure 5b. Thus, trehalose has no noticeable effect on the UV-excited fluorescence of this bioconjugate but the intensity of Ag^0·PE fluorescence excited by visible light increases in the entire fluorescence spectrum by 40% to 20%±3% depending on the excitation wavelength. The fluorescence intensity of Ag^0·PE is enhanced by the fact that the distance between Ag^0 NP and the terminal excitation energy acceptor in R-phycoerythrin (β84PEB) located on the surface of the tunnel cavity decreases as a result of water binding by trehalose. In addition, the intensity of Ag^0 NP fluorescence is enhanced as a result of the surfaces plasmon resonance.

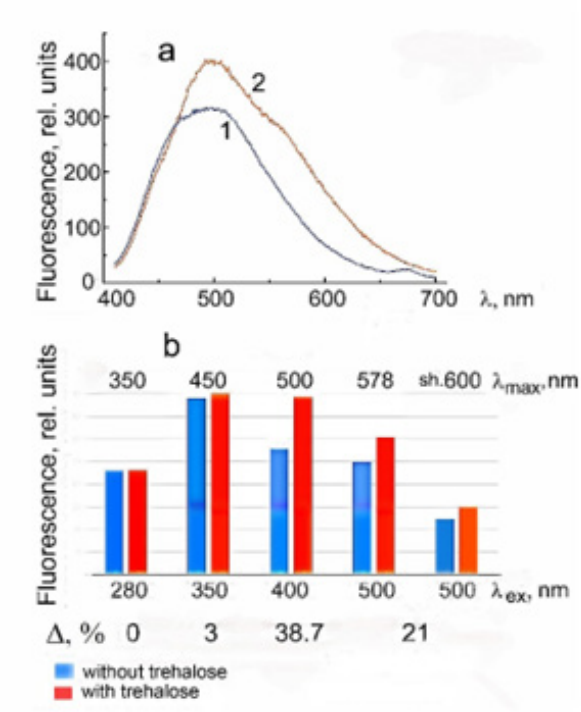

Figure 5: (a) Fluorescence emission spectrum of Ag^0·PE in ultrapure water (curve 1) in the absence of trehalose and (curve 2) in the presence of 0.73M trehalose excited at 400nm. (b) The effect of trehalose on the fluorescence emission of Ag^0·PE in maxima at 350nm (Trp), 450nm and 500nm (Ag^0 NPs), 578nm and a shoulder at 600nm (R-phycoerythrin) excited at 280, 350, 400, and 500nm. Δ, %, are changes in the entire fluorescence spectrum of Ag^0·PE after exposure to trehalose.

Optical properties of CdS·PE bioconjugate

Figure 6 shows the absorption spectrum of CdS·PE and its second derivative. The absorption edge corresponds to small-sized CdS NPs. The minimum at 444nm in the second derivative of the spectrum corresponds to the absorption maximum of CdS NPs with a diameter of 3.5nm±5%. The band gap (exciton energy) of the NPs in CdS·R-PE is 2.8eV. This is the value at which crystalline materials with a semiconductor energy structure exhibit photocatalytic properties [29,34,36]. The size of 3.5nm is equal to the diameter of the tunnel cavity in R-phycoerythrin (the site of NP synthesis). The minimum is indistinct at 480nm in the second derivative spectrum, corresponding to the NP size of 6.0nm (equal to the length of the tunnel cavity), is vague. This is attributed to the hypochromic effect and the inverse dependence of absorbance on the particle size (the larger the size, the smaller the extinction coefficient). The CdS·PE bioconjugate strongly absorbs in the UV and blue spectral regions, whereas the absorption peaks characteristic of native R-phycoerythrin (at 498, 540, and 568nm) are poorly distinguishable, (Figure 6, curve 1). This is due to changes in the configuration of chromophore groups and conformational mobility of R-phycoerythrin that occurred in the course of nanoparticle synthesis. In the presence of 0.73M trehalose, the CdS·PE absorption is slightly enhanced, but the position of its edge remains unchanged, indicating that trehalose has no effect on the size of CdS NPs, (Figure 6, curve 2).

Copyright © Bekasova OD

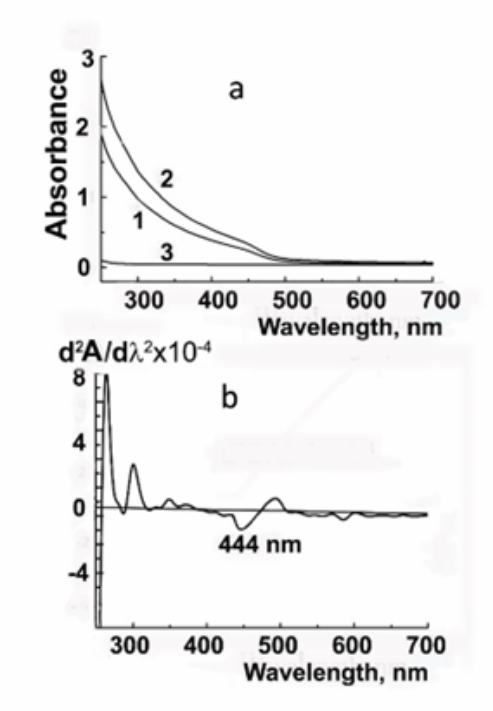

Figure 6: (a) Absorption spectra of CdS·PE in ultrapure water (0.12mg/mL): (1) in the absence of trehalose, (2) in the presence of 0.73M trehalose and (3) of 0.73M trehalose alone (b) Second derivatives of the absorption spectra of CdS·PE.

The fluorescence spectra of CdS·PE recorded at different excitation wavelengths (λ_{ex}) are shown in Figure 7. The spectrum has two peaks in the visible light range: one for R-phycoerythrin at 578nm and the other for CdS NPs at 450nm (λ_{ex}=350nm) or at 480-500nm (λ_{ex}=400nm). The intensity of R-phycoerythrin fluorescence excited at 500nm is an order of magnitude higher, because this excitation length is in the overlap region between the absorption band of R-phycoerythrin and the fluorescence maximum of CdS NPs. The fluorescence spectrum excited at 280nm has three bands assigned to tryptophan (350nm), CdS NPs (440nm), and R-phycoerythrin (578nm), (Figure 8). The effect of trehalose on the fluorescence of CdS·PE is ambiguous. Thus, in presence of trehalose, the fluorescence excited by visible light increases by 20%, while the fluorescence excited at 280nm, on the contrary, decreases by about a half, *cf.* Figures 7 & 8. In addition to the decrease in the fluorescence intensity, all emission peaks are shifted by 10nm to longer wavelengths. In particular, the peak at 570nm is shifted to 578nm and its half-width increases from 32 to 36nm. The distribution of fluorescence intensity excited at 280nm also changes in the absence of trehalose, the main peak of NPs is at 440nm (F_{max} 440>F_{max} 350≥F_{max}570nm), while the dominant fluorescence in the presence of trehalose is that of tryptophan, with a maximum at 360nm (F_{max}360>F_{max}450>F_{max}578nm). The changes in the position of the maxima and a decrease in the intensity throughout the fluorescence spectrum excited at 280nm indicate that the energy migration in the CdS·PE bioconjugate is impaired under the influence of trehalose.

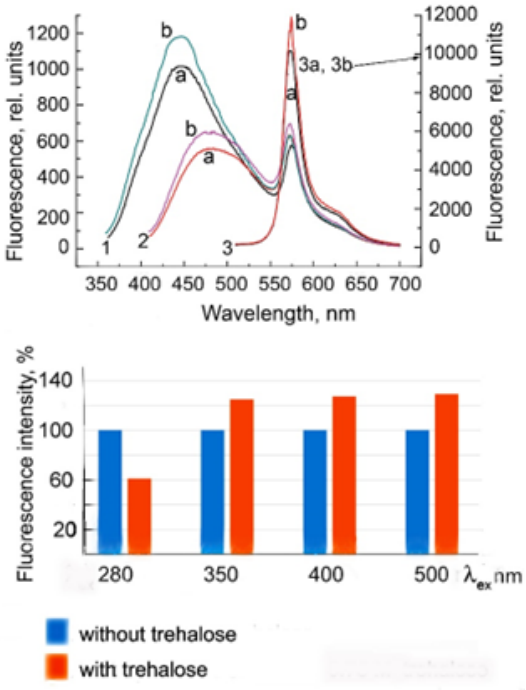

Figure 7: Fluorescence emission spectra of CdS·R-PE excited at (1) 350nm, (2) 400nm, (3) 500nm (a) in the absence of trehalose and (b) in the presence of 0.73M trehalose and the patterns of changes in the fluorescence spectrum of a bioconjugate excited by light of different wavelengths. The fluorescence intensity in the absence of trehalose was taken as 100%.

Copyright © Bekasova OD

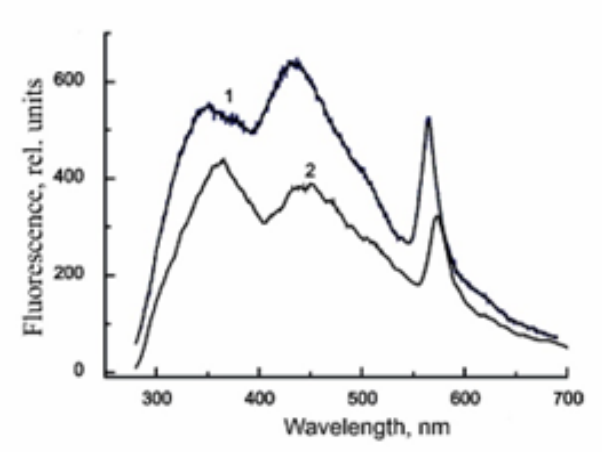

Figure 8: Fluorescence emission spectra of CdS·PE (1) in the absence of trehalose and (2) in the presence of 0.73M trehalose excited at 280nm.

The intensity of CdS·PE fluorescence excited by visible light increases in the presence of trehalose due to enhancement of the intrinsic fluorescence of R-phycoerythrin and CdS NPs. Wherein the intrinsic fluorescence of R-phycoerythrin enchancement by the partial elimination of defects on the surface of the R-phycoerythrin molecule, mainly on its structural sites adjacent to chromophore groups in the β-subunits: β50/61PUB and β155 PEB, the main light harvesters located on the outside surface of R-phycoerythrin and β84PEB terminal acceptor, located on the surface of R-phycoerythrin tunnel cavity. The intrinsic fluorescence of CdS NP is enhanced because weaken of its connection with R-phycoerythrin in the presence of trehalose.

Influence of trehalose on the photovoltaic effect in CdS·PE films

Figure 9, curve 1 shows changes in the potential of a platinum electrode coated with an R-phycoerythrin film that is immersed in ethanol containing dissolved oxygen. This potential remains unchanged in the dark, decreases when the light is on, and returns to the initial level (or close to it) when the light is off. Such changes may be observed repeatedly, with their amplitude and time course remaining the same. A characteristic feature of phycobilin pigments, including R-phycoerythrin, is that they produce a negative photo potential (PP) under both oxidizing and reducing conditions. The photo potential is the difference between the potentials of the platinum electrode and the standard calomel electrode recorded in the light and in the dark, i.e., it characterizes reversible changes in the system under these conditions. CdS·PE films prepared on the platinum electrode have a positive PP in the light, as opposed to R-phycoerythrin films (Figure 9, curve 2). When the light is switched on, their PP increases rapidly (in some cases up to +250mV) and reaches a maximum after 1.5-2min; as the light is off, the potential changes in the opposite direction and approaches the initial level within a few minutes. Such a pattern of changes, with the same amplitude and time course, can be observed repeatedly, as in R-phycoerythrin films. As shown in our previous study [29], high PP values in CdS·PE films and rapid reversibility of the changes in PP under light switching on and off are due to the photosensitizing action of R-phycoerythrin. The sensitized photo effect is significantly higher than the photoelectric sensitivity of R-phycoerythrin and has the opposite polarity.

The film prepared from a CdS·PE solution in water in the presence of trehalose produce a negative PP, like in the films prepared from native R-phycoerythrin, but the PP amplitude is lower. The presence of CdS NP in CdS·PE is not manifested under these conditions (Figure 9, curve 3). Probably, trehalose inhibits the photosensitizing ability of R-phycoerythrin. A significant decrease in the PP value in the presence of trehalose under oxidizing conditions may be due to a change in the rate of O_2 reduction at the interface between the CdS·PE film and the electrolyte as a result of water binding by trehalose. This suggestion is confirmed by the fact that the photovoltaic effect is inhibited in a two-layer film of trehalose/CdS·PE, prepared by spraying a solution of trehalose onto the CdS·PE film followed by drying of the solution of trehalose, Figure 9, curve 4. The abrupt change in PP may also be facilitated due to the surface roughness of the film that formed in the presence of trehalose [36].

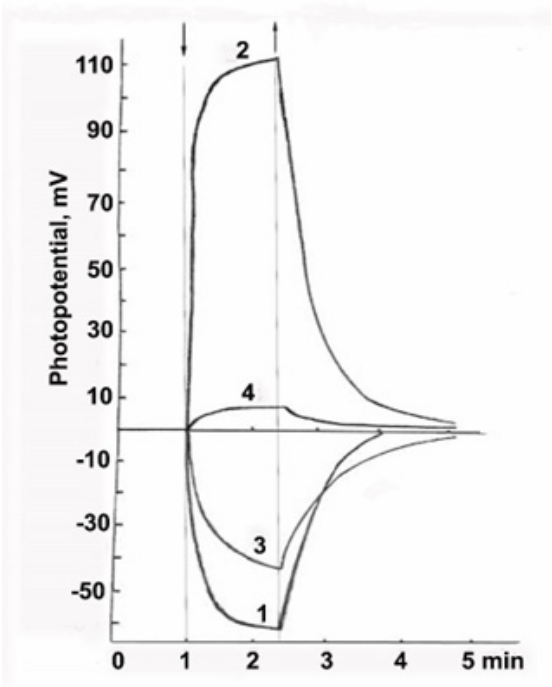

Figure 9: Changes in the photo potential of the films prepared from water solutions of (1) R-phycoerythrin, (2) CdS·PE, (3) CdS·PE in the presence of trehalose and (4) a trehalose-CdS·PE bilayer film. The measurements were performed in the presence of atmospheric oxygen. (↓), light on; (↑), light off.

Discussion

According to our previous observations, both reversible and irreversible changes in R-phycoerythrin take place in the course of NP synthesis [15,17,28,37]. The correlation between the Ag^0·PE and CdS·PE fluorescence spectra and the structural properties of R-phycoerythrin and NPs allows us to detect structural changes of R-phycoerythrin that occur during NP synthesis in the pigment

Copyright © Bekasova OD

cavity as well as during trehalose exposure to bioconjugates. In solutions, the chromophore groups of R-phycoerythrin may adopt various configurations, from porphyrin-type cyclic structures to elongated [38]. The elongated conformation is associated with strong absorption in the bands with maxima at 496, 540, 564nm. The high quantum yield of fluorescence is characteristic of native R-phycoerythrin. Bilins in cyclohelical conformations are characterized by a weak absorption band in the visible region of the spectrum, strong absorption in the UV spectral region, and weak fluorescence are characteristic of denatured *R*-phycoerythrin [39]. The fact that trehalose does not affect the absorption spectrum of Ag^0·PE and its fluorescence spectrum excited at 280nm suggests that trehalose does not affect the configuration of the chromophores and the interaction between the chromophores and protein residues in the Ag^0·PE bioconjugate. In this regard, the increase in the fluorescence intensity of the Ag^0·PE bioconjugate upon direct excitation of the chromophore groups or Ag^0·NPs, i.e., upon excitation with visible light, is most likely due to the fact that water binding by trehalose causes a decrease in the distance between the R-phycoerythrin chromophores and Ag^0·NPs, which in turn facilitates the excitation energy transfer and enhancement of Ag^0·PE fluorescence excited by visible light at 400, 450, and 500nm. It also cannot be ruled out that water, binding by trehalose and shorter interactions between NPs and chromophore groups, affects the surface of NPs and, as a consequence, the fluorescence of Ag^0 NPs is enhanced by increasing the surface plasmon resonance fluorescence.

In contrast to Ag^0·PE, the CdS·PE fluorescence excited at 280nm in the presence of trehalose decreases across the spectrum by about a half and the Trp fluorescence dominates with a maximum at 360nm. This fact confirms the reduction in energy migration from aromatic amino acids to chromophores of R-phycoerythrin. The fluorescence properties of Trp residues are very sensitive to their microenvironment [40]. This suggests that trehalose may increase the intramolecular mobility of the indole ring by causing a conformational change in the Trp side chain, thereby bringing the indole ring closer to the CdS NP. Due to the reduction of this distance and the ability of the CdS NP to generate high-potential electron-hole pairs upon excitation, electron detachment from the indole ring occurs under illumination, i.e., when the Trp residue and CdS NP are in the excited state. This is confirmed by the CdS·PE photovoltaic effect and a decrease in the intensity of CdS·PE fluorescence excited at 280nm. This interpretation is consistent with the fact that trehalose has no effect on the UV-excited fluorescence of the Ag^0·PE bioconjugate (Ag^0 carries no charge and therefore cannot detach an electron from the indole ring of the Trp residue upon its excitation). Thus, the ambiguous effect of trehalose on the UV-excited fluorescence of the Ag^0·PE and CdS·PE bioconjugates is due to the unequal nature of NPs (metal and semiconductor).

Conclusion

In conclusion, using two photosensitive R-phycoerythrin bioconjugates similar in size but differing in the nature of NPs. In the presence of trehalose, the fluorescence of Ag^0·PE and CdS·PE bioconjugates enhanced only upon direct excitation of R-phycoerythrin chromophores and NPs. However, the mechanisms of their fluorescence enhancement are different. It was shown that trehalose enhances the interaction of Ag^0 NPs with chromophores by reducing the distance between them. In addition, the intensity of Ag^0 NP fluorescence is enhanced as a result of the surfaces plasmon resonance. But trehalose does not eliminate defects in the R-phycoerythrin structure arising in the course of Ag^0 NPs synthesis; in other words, trehalose does not affect the configuration of chromophores and their interactions. The intensity of CdS·PE fluorescence excited by visible light increases in the presence of trehalose due to enhancement of the intrinsic fluorescence of R-phycoerythrin and CdS NPs. Wherein the intrinsic fluorescence of R-phycoerythrin enchancement by the partial elimination of defects on the surface of the R-phycoerythrin molecule, mainly on its structural sites adjacent to chromophore groups, the main light harvesters located on the outside surface of R-phycoerythrin and β84PEB terminal acceptor, located on the surface of R-phycoerythrin tunnel cavity. The intrinsic fluorescence of CdS NP is enhanced because weaken of its connection with R-phycoerythrin in the presence of trehalose.

Potentiometric studies of the photochemical activity of CdS·PE showed that trehalose inhibits photosensitizing ability of R-phycoerythrin. This means that trehalose can suppress the ability of dyes to sensitize photoelectric processes in semiconductors. Therefore, trehalose cannot be used to develop electrochemical biosensors based on semiconductors. The mechanism of fluorescence amplification of R-phycoerythrin, Ag^0·PE, and CdS·PE excited by visible light was elucidated based on the fluorescence spectroscopy analysis of the effect of trehalose on the fluorescence of both bioconjugates. The results of this study demonstrate that trehalose can be successfully used for the efficient optimization of bioactive materials and their fine tuning to create optical biosensors for diagnosis and monitoring diseases, drug discovery. An enhanced fluorescence intensity of Ag^0·PE and CdS·PE bioconjugates excited by visible light is particularly important for their future applications in nanomedicine based on single-molecule nanostructures.

Acknowledgement

I gratefully acknowledge financial support from the Ministry of Science and Higher Education of the Russian Federation. I thank Professor Boris I. Kurganov for his interest in this study and discussion of the results.

Compliance with Ethical Standards

All studies were conducted in accordance with ethical standards.

References

1. Quinten M (2011) Optical Properties of Nanoparticle Systems: Mie and beyond. Wiley, Germany.
2. Turner APF (2000) Biosensors-sense and sensitivity. Science 290(5495): 1315-1317.
3. Mukherjee S, Chowdhury D, Kotcherlakota R, Sujata P, Vinothkumar B, et al. (2014) Potential theranostics application of bio-synthesized silver nanoparticles (4-in-1 system). Theranostics 4(3): 316-335.

Copyright © Bekasova OD

4. Chen D, Wang G, Li J (2007) Interfacial bioelectrochemistry: Fabrication, properties, and applications of functional nanostructured biointerfaces. J Phys Chem 111(6): 2351-2367.
5. Salih NA (2013) The enhancement of breast cancer radiotherapy by using silver nanoparticles with 6MeV Gamma photons. Advances in Physics Theories and Applications 26: 10-12.
6. Glaser AN (1989) Light guides: Directional energy transfer in a photosynthetic antenna. J Biol Chem 264(1): 1-4.
7. Chang WR, Jiang T, Wan ZL, Zhang JP, Yang ZX, et al. (1996) Crystal structure of R-phycoerythrin from polysiphonia urceolata at 2.8A resolution. J Mol Biol 262(5): 721-731.
8. Jiang T, Zhang J, Liang D (1999) Structure and function of chromophores in R-phycoerythrin at 1.9A resolution. Proteins 34(2): 224-231.
9. Dmitrievskii OD, Ermolaev VL, Terenin AN (1957) Direct lifetime measurements for excited chlorophyll and similar pigment molecules in various media. Dokl Akad Nauk SSSR 114: 751-753.
10. He JA, Hu YZ, Jiang LJ (1997) Photodynamic action of phycobiliproteins: *In situ* generation of reactive oxygen species. Biochimica et Biophysica Acta (BBA)-Bioenergetics 1320(2): 165-174.
11. Sudhakar MP, Jagatheesan A, Perumal K, Arunkumar K (2015) Methods of phycobiliprotein extraction from *Gracilaria Crassa* and its applications in food colorants. Algal Research 8: 115-120.
12. Huang B, Wang G, Zeng C, Li Z (2002) The experimental research of R-phycoerythrin subunits on cancer treatment: A new photosensitizer in PDT. Cancer Biother Radiopharm 17(1): 35-42.
13. Batard P, Szollosi J, Luescher I, Cerrottini JC, MacDonald R, et al. (2002) Use of phycoerythrin and allophycocyanin for fluorescence resonance energy transfer analysed by flow cytometry: Advantages and limitations. Cytometry 48(2): 97-105.
14. Isailovic D, Sultana I, Phillips GJ, Yeung ES (2006) Formation of fluorescent proteins by the attachment of phycoerythrobilin to R-phycoerythrin alpha and beta apo-subunits. Analytical Biochemistry 358(1): 38-50.
15. Bekasova OD, Brekhovskikh AA, Brykina GD, Dubinchuk BT, Mochalova VS, et al. (2005) R-Phycoerythrin: A natural ligand for detoxifying cadmium ions and a tunnel matrix for synthesis of cadmium sulfide nanoparticles. Appl Biochem Microbiol 41: 269-274.
16. Brekhovskikh AA, Bekasova OD (2005) CdS nanoparticles in R-phycoerythrin, a protein matrix. Inorg Mater 41: 331-337.
17. Bekasova OD, Brekhovskikh AA, Revina AA, Dubinchuk BT (2008) Preparation and optical properties of silver nanoparticles in R-phycoerythrin, a protein matrix. Inorg Mater 44: 835-841.
18. Bekasova OD, Kurganov BI (2021) Bioconjugate of R-phycoerythrin with Ag^0 nanoparticle-functional nanostructure for cancer theranostics, fluorescent biosensors and electrochemical biointerfaces. International Congress Biotechnology: State of the Art and Perspectives 26-29(19): 73-75.
19. Bekasova OD, Borzova VA, Shubin VV, Kovalyov LI, Stein-Margolina VA, et al. (2016) An increase in the thermal stability of R-phycoerythrin by silver nanoparticles synthesized in nanochannels of the pigment. Appl Biochem Microbiol 52: 98-104.
20. Bekasova OD, Stein-Margolina VA, Kurganov BI (2018) Ag^0 nanoparticles synthesized in R-phycoerythrin: Change in bioconjugate properties upon ripening of nanoparticles. Curr Pharm Biotechnol 19(5): 422-427.
21. Bekasova OD, Ryvkina NG, Chmutin IA, Shtein-Margolina VA, Kurganov BI (2017) Electrical properties of R-phycoerythrin containing Ag^0 nanoparticles in its channels. Inorg Mater 53: 1249-1253.
22. Mahendia S, Tomar AK, Kumar S (2010) Electrical conductivity and dielectric spectroscopic studies of PVA-Ag nanocomposite films. J Alloys Com 508(2): 406-411.
23. Mutiso RM, Winey KI (2015) Electrical properties of polymer nanocomposites containing rod-like nanofillers. Prog Polym Sci 40: 63-84.
24. Mukherjee S, Chowdhury D, Kotcherlakota R, Sujata P, Vinothkumar B, et al. (2014) Potential theranostics application of bio-synthesized silver nanoparticles (4-in-1 system). Theranostics 4(3): 316-335.
25. Ovais M, Khalil AT, Raza A, Khan MA, Ahmad I, et al. (2016) Green synthesis of silver nanoparticles via plant extracts: Beginning a new era in cancer theranostics. Nanomedicine 11(23): 3157-3177.
26. Choi YJ, Gurunathan S, Kim JH (2018) Graphene oxide-silver nanocomposite enhances cytotoxic and apoptotic potential of salinomycin in human ovarian cancer stem cells (OvCSCs): A novel approach for cancer therapy. Int J Mol Sci 19(3): 710-733.
27. Bekasova OD, Rusanov AL (2010) Dynamics of silver nanoparticle fluorescence in the R-phycoerythrin molecule. Dokl RAS 430(2): 208-211.
28. Bekasova OD, Chebotareva NA, Safenkova IV, Rusanov AL, Kurganov BI (2011) Effect of CdS nanoparticles on the properties of a protein matrix. Inorg Mater 47: 830-836.
29. Bekasova OD, Revina AA, Kornienko ES, Kurganov BI (2015) The photovoltaic effect of CdS quantum dots synthesized in inverse micelles and R-phycoerythrin tunnel cavities. Appl Biochem Biotechnol 176: 1141-1150.
30. Robel I, Bunker BA, Kamat PV (2005) Single-walled carbon nanotube-CdS nanocomposites as light-harvesting assemblies: Photoinduced charge-transfer interactions. Adv Mater 17(20): 2458-2463.
31. Eronina TB, Mikhaylova VV, Chebotareva NA, Shubin VV, Sluchanko NN, et al. (2019) Comparative effects of trehalose and 2-hydroxypropyl-β-cyclodextrin on aggregation of UV-irradiated muscle glycogen phosphorylase b. Biochimie 165: 196-205.
32. https://www.taylorfrancis.com/books/mono/10.1201/9781351075565/phycobiliproteins-robert-maccoll-deborah-guard-friar
33. Bradford MM (1976) A rapid and sensitive method for the quantitation of microgram quantities of protein utilizing the principle of protein-dye binding. Anal Biochem 72: 248-254.
34. Wang Y, Herron N (1991) Nanometer-sized semiconductor clusters: Materials synthesis, quantum size effects, and photophysical properties. J Phys Chem 95(2): 525-532.
35. Alqudami A, Annapoorni S (2007) Fluorescence from metallic silver and iron nanoparticles prepared by exploding wire technique. Plasmonics 2: 5-13.
36. Atakulov SB, Zainolobidinova SM, Nabiev GA, Tukhtamatov OA (2012) Effect of the structural features of polycrystalline semiconductor films on the formation of anomalous photo-voltage: II Comparison with experiment. Semiconductors 46: 714-718.
37. Bekasova OD, Shubin VV, Safenkova IV, Kovalyov LI, Kurganov BI (2013) Structural changes in R-phycoerythrin upon CdS quantum dot synthesis in tunnel cavities of protein molecules. Int J Biol Macromol 62: 623-628.
38. Scheer H (1981) Biliproteins. Angew Chem Int Ed Engl 20(3): 241-261.
39. Glazer AN (1982) Phycobilisomes: Structure and dynamics. Ann Rev Microbiol 36: 173-198.
40. Hixon J, Reshetnyak YK (2009) Algorithm for the analysis of tryptophan fluorescence spectra and their correlation with protein structural parameters. Algorithms 2(3): 1155-1176.

For possible submissions Click below:

Submit Article

Copyright © Bekasova OD